Available online at www.sciencedirect.com
ScienceDirect
Atmospheric Environment 41 (2007) 4227–4241
ATMOSPHERIC ENVIRONMENT
www.elsevier.com/locate/atmosenv

Nitric acid and the origin and size segregation of aerosol nitrate aloft during BRACE 2002

J.R. Arnold[a,*,1], Winston T. Luke[b]

[a]*Atmospheric Sciences Modeling Division, National Oceanic and Atmospheric Administration, Air Resources Laboratory, 1200 6th Avenue/9th FL/OEA-095, Seattle, WA 98101-1128, USA*
[b]*Air Resources Laboratory, National Oceanic and Atmospheric Administration, Silver Spring, MD, USA*

Received 9 February 2006; received in revised form 19 July 2006; accepted 21 July 2006

Abstract

As part of the BRACE 2002 May field intensive, the NOAA Twin Otter flew 21 missions over terrestrial, marine, and mixed terrestrial and marine sites in the greater Tampa, Florida, airshed including over Tampa Bay and the Gulf of Mexico. Aerosols were collected with filter packs and their inorganic fractions analyzed post hoc with ion chromatography. Anion mass dominated both the fine- (particle diameters $\leqslant 2.5\,\mu m$) and coarse-mode (particle diameters 10.0–2.5 μm) inorganic fractions: SO_4^{2-} in the fine fraction, $3.7\,\mu g\,m^{-3}$ on average and Cl^- and NO_3^- in the coarse fraction, $0.6\,\mu g\,m^{-3}$ on average and $1.4\,\mu g\,m^{-3}$ on average, respectively. Ammonium ion dominated the inorganic fine-mode cation mass, averaging $1.2\,\mu g\,m^{-3}$, presumably in association with SO_4^{2}. Coarse-mode cation mass was dominated by Na^+, but the concentrations of Ca^{2+} and K^+ together often equaled or exceeded the Na^+ mass which was, on average, $0.6\,\mu g\,m^{-3}$. Nitrate appeared predominantly in the coarse rather than the fine fraction, as expected, and the fine fraction never contributed >15% of the total NO_3 concentration. Nitric acid dominated the NO_3^- contribution from both aerosol size fractions, and constituted at least 45% of the total NO_3 in all samples. Coarse-mode Cl^- depletion, and hence NO_3^- replacement, reached 100% within the first 4 h of plume travel from the urban core in some samples, although it was most often less than 100% and slightly below the expected 1:1 ratio with coarse-mode NO_3^- concentration: the slope of the regression line of NO_3^- concentration to Cl^- depletion was 0.9 in the coarse fraction. In addition, terrestrial samples were markedly lower in Cl^- depletion, and thus in substituted NO_3^-, than were marine and mixed samples: 15–25% depletion in terrestrial samples vs. 50–65% in marine samples with the same air mass age. Thus, we conclude that NO_3^- and its progenitor compound HNO_3 were present in the Tampa airshed in insufficient amounts to titrate fully the slightly alkaline coarse-mode particles there, and to replace completely the Cl^- from the coarse-mode NaCl.
Published by Elsevier Ltd.

Keywords: Sea salt; Chloride depletion; Nitrate limitation; Aerosol constituents; Coastal ecosystems

1. Introduction

1.1. Atmospheric production of reactive nitrogen

Human output of reactive nitrogen (N) from production of energy and food now exceeds the

*Corresponding author. Tel.: +206 553 8579; fax: +206 553 8210.
E-mail address: arnold.jeff@epa.gov (J.R. Arnold).
[1]In partnership with the National Exposure Research Laboratory, Office of Research and Development, U.S. Environmental Protection Agency.

1352-2310/$ - see front matter Published by Elsevier Ltd.
doi:10.1016/j.atmosenv.2006.07.059

yields from lightning, bacterial fixation, and all other natural sources (Galloway et al., 2003), an increase that has overwhelmed the natural processes which remove it through denitrification to N_2. The accumulation of reactive N that results has complex negative consequences in the bio-, atmo-, and hydrosphere. On land, anthropogenic N acidifies soils, displacing other nutrients and changing species composition and biodiversity in forests and grasslands. In the atmosphere, nitrogen oxides ($NO_X = NO + NO_2$), chiefly from fossil fuel combustion, lead to production of ozone (O_3), aerosols, and acid rain in the troposphere, to the depletion of O_3 in the stratosphere, and contribute directly and indirectly to global warming and climate change. In the hydrosphere, reactive N from direct sources or deposited from the atmosphere can contaminate ground water, acidify freshwater lakes, streams, and rivers, and produce eutrophic conditions in estuaries and other coastal waters with concomitant loss of sheltering sea grasses and the higher biota supported there (UNEP, 2004; Howarth et al., 2000). Such changes in estuaries and shallow coastal waters may have significant global effects since roughly half of global oceanic primary production is estimated to come from these sites (Paerl, 1995).

An appreciable fraction of the reactive N loadings to critical ecosystems like estuaries comes from the atmospheric deposition of N pollutants, most derived from the NO_X released in fossil fuel combustion for power generation, transportation, and industrial processes. In the troposphere, NO participates in a complex chain of oxidizing chemical reactions driven by ultraviolet light and involving hydrocarbons. Intermediate and end products from this oxidizing chain include a series of odd oxygen (O_X) compounds, where O_X is the category label of all species that can act as reservoirs for atomic oxygen, primarily O_3, NO_2, nitric acid (HNO_3), and peroxyacetyl nitrate (PAN), with minor contributions from short-lived radical species like the nitrate ion (NO_3^-) and from higher organic nitrates ($RONO_2$).

The primary mechanism for odd oxygen production ($P(O_X)$) in the troposphere is the oxidation of NO to NO_2 by the hydroxy (OH) and peroxy (HO_2 and RO_2) radicals as in (R1) and (R2):

$$HO_2 + NO \rightarrow OH + NO_2, \quad (R1)$$

$$RO_2 + NO \rightarrow RO + NO_2. \quad (R2)$$

The NO_2 thus formed can then photolyze, returning the original NO as in (R3), or can undergo OH attack as in (R4):

$$NO_2 + h\nu \rightarrow NO + O(^3P), \quad (R3)$$

$$OH + NO_2 \rightarrow HNO_3. \quad (R4)$$

(R3) propagates $P(O_X)$ while (R5) terminates the reaction series by producing HNO_3, an end product that is largely stable in the troposphere on urban and regional time scales. Nitric acid adsorbs strongly to surfaces, is highly soluble in water and easily incorporated into aerosols, and can directly deposit to surfaces from the gas phase with a deposition velocity (V_d) at the limit of aerodynamic resistance, 1–5 $cm^2\,s^{-1}$. Thus, its lifetime in the troposphere is short, and HNO_3 constitutes the primary sink for NO released to the atmosphere.

1.2. Atmospheric reactive nitrogen in critical estuarine ecosystems

Acidic gas-phase species like HNO_3 in marine environments can be converted to solid or aqueous phase in reaction with solid or liquid sea salt aerosols. The presence of these particulate surfaces for heterogeneous reactions is significant both locally for marine ecosystems and more globally: sea salt's aggregate surface area over a given location represents from 1 to 10% on an annual average of the area of the underlying Earth's surface (Guelle et al., 2001), and 21% of the total column global aerosol surface area (Guelle et al., 2001). Gas- to solid-phase conversion of NO_3^- preferentially partitions HNO_3 in the marine environment onto these more prevalent coarse particles (particle diameters 10.0–2.5 μm), rather than into the fine-mode fraction (particle diameters $\leqslant$2.5 μm) typically encountered over terrestrial locations. The effect of this NO_3^- size segregation can be to increase the local N deposition, since coarse particles have much higher settling velocities than smaller ones, and to deplete the sea salt aerosol of Cl^-, since the HCl created by uptake of HNO_3 on the particle surface, as in (R5), volatilizes very efficiently (Mamane and Mehler, 1987; Clarke et al., 1999, Zhang et al., 1999):

$$HNO_{3(g)} + NaCl_{(p)} \leftrightarrow HCl_{(g)} + NaNO_{3(p)}. \quad (R5)$$

But NaCl is not the sole marine aerosol component, of course, and reactions analogous to (R5) occur with $CaCl_2$, KCl, and $MgCl_2$ as well. This set of N

reactions with aerosol salts in marine atmospheres (reviewed by De Haan et al., 1999) is important not only for halogen cycling and oxidation reactions (Andreae and Crutzen, 1997) but also because through them NO_3 can be shifted from gas-phase HNO_3 or from fine-mode aerosol (after dissociation of NH_4NO_3, for example) to coarse-mode particles, thereby enhancing the potential for local N deposition in coastal regions. The actual area extent of N deposition resulting from gas-to-particle NO_3 conversion is, however, a complex function of local wind speeds, as shown by Pryor and Sørensen (2000): with moderate winds of 3.5–10 m s^{-1}, HNO_3 V_d exceeds that of an average $NaNO_3$ particle, whereas at higher and lower wind speeds the reverse is true. This means that as a result of gas-to-particle NO_3 conversion, under commonly moderate winds, less N would be deposited locally and more would be available for transport and deposition in a larger area of extent.

Atmospheric inputs of reactive N to coastal waters are essentially equal to those contained in riverine inflow (Duce et al., 1991) and may contribute from 20% to more than 50% of external N loadings to these systems (Paerl, 1997). Estimates of the atmospheric fraction of riverine reactive N carried to coastal waters in the eastern US range from 36% to 80% (Jaworski et al., 1997). In Chesapeake Bay, for example, direct deposition of atmospheric NO_3 may contribute 20–30% of the N total and 14% of the NH_4^+ loading (Fisher and Oppenheimer, 1991). For Tampa Bay, estimates of the direct atmospheric contribution to the Bay's total N loading range from 21% to 24% of the ~3500 metric tons of N reaching the Bay each year, with slightly more than half of the atmospheric fraction coming as wet deposition (Prible et al., 2003; Poor et al., 2001).

Eutrophication resulting from this excess N in Tampa Bay has been in large part responsible for the ~40% die-off of the Bay's seagrass meadows since 1950 (Prible et al., 2003) and for the marked decline in higher biota these grasses support. Human population in the urban centers surrounding the Bay exceeds two million, producing an estimated 547 t day^{-1} of NO_X emissions in 1990 (FDEP, 2002). That total is projected to have fallen to 254 t day^{-1} in 2005 when significant controls and re-powering at fossil-fueled power plants directly adjacent to the Bay will have lowered the projected point source NO_X emissions from 58% of the 1990 total to 25% of the projected 2005 total. Both the absolute and relative effects from this source change are significant for the air- and watershed. The new projected totals, for example, will reduce point source NO_X to less than half of the projected 2005 total for on- and off-road mobile source emissions (FDEP, 2002).

The scale of these N loads and the projected changes in total NO_X emissions and in source apportionment around Tampa Bay presented an especially useful opportunity to research the sources, transformation, and fate of atmospheric N in critical estuaries. As part of the Bay Regional Atmospheric Chemistry Experiment (BRACE) field intensive in May 2002 (see Atkeson et al., 2007, for an overview), the NOAA Twin Otter aircraft flew 21 research missions in the greater Tampa region over urban, suburban, and rural areas, and over Tampa Bay and the Gulf of Mexico (see Luke et al. (this issue), for a detailed discussion of the Twin Otter research objectives). We report here on results from aircraft samples taken on missions flown during each of the four flow regimes that predominated during the BRACE 2002 intensive: strong synoptic, when local effects were overwhelmed; synoptic shift, with wind shifts due to changing synoptic features; and strong or weak sea and/or bay breeze, when local effects of the Gulf and Bay forced wind shifts. Findings from these flights will be used in the larger BRACE project efforts in three ways: to help characterize the size segregation of NO_3 in Tampa Bay coastal areas and the role of sea salt in determining that partitioning as done here; with future deposition estimates for the Bay and the wider Tampa airshed; and for testing photochemical grid model predictions made for the Tampa airshed and a larger southeast US domain still to be completed.

2. Instrumentation

We refer the reader to Luke et al. (this issue) for a detailed discussion of the Twin Otter measurement platform including the gas- and particle-phase sampling methods and apparatus. Here, we give simply an outline of some elements directly significant for the HNO_3 results. The BRACE aircraft missions generally lasted for the full duration of the Twin Otter's research flight interval, 4.5 h, most often during the period of the day with highest photochemical production, 10:00–14:00 LT, and were augmented with a second flight on days with

favorable conditions. Sampling was conducted in the range of 100–3000 m above ground level.

2.1. Teflon-coated aerosol inlet and manifold for inorganic aerosols

The Twin Otter aerosol inlet used for this work is a forward facing, shrouded isokinetic sampling probe mounted with its longitudinal axis 14 cm above the aircraft fuselage. To minimize adsorption of reactive trace gases and particles, the probe tip and inlet assembly are coated with a highly cross linked Teflon surface, as is the sampling manifold inside the Twin Otter cabin. Each of five ports on the manifold can be mated to a variety of filter packs (FPs) and denuder systems manufactured by University Research Glassware (URG, Carrboro, NC).

2.2. Filter pack measurements of inorganic aerosols

Two two-stage URG FPs (URG P/N URG-2000-30FG) were used to collect inorganic aerosols in both fine ($d<2.5\,\mu m$) and bulk ($d<\sim10\,\mu m$) size fractions. Each FP assembly consisted of a PTFE Teflon-coated 1 μm prefilter (Whatman P/N 7590-004) and a backup cellulose filter (Whatman P/N 1441-047) impregnated with a solution of 1% NaCl in 65/20/15 water/methanol/glycerol for the collection of gas-phase HNO_3. Teflon filters were extracted in 10 ml of a solution of 10% MeOH in $>18\,M\Omega$ H_2O; cellulose filters were extracted in 10 ml of $>18\,M\Omega$ H_2O and stored under refrigeration.

Analysis was performed at the University of South Florida where the filter extracts were analyzed for major ions with a Dionex DX-600 ion chromatograph. Check standards remained within 5% of the expected concentrations and reproducibility of regularly introduced duplicate samples was within 3%.

We report results for the fine-mode samples directly measured and for a coarse-mode fraction ($2.5<d<\sim10\,\mu m$) computed as the difference between the measured bulk size fraction and the measured fine-mode fraction.

3. Results

3.1. Meteorological conditions during BRACE

Synoptic conditions in Tampa during May 2002 diverged from climatological means, holding stronger than expected and frequently overwhelming the set-up of local sea- and bay-breezes. On average, the 500 mb geopotential heights were ~40 m higher than usual (NOAA–CIRES/Climate Diagnostic Center), producing stronger subsidence and warmer air and suppressing convection. A stronger surface pressure gradient persisted throughout the southeast US during this period (NOAA–CIRES/Climate Diagnostic Center), increasing the NE wind component at Tampa by $\sim2\,m\,s^{-1}$ and thereby suppressing regular formation of the westerly sea-breezes. With stronger winds and temperatures generally $<1\,^{\circ}C$ above average, normal convection was effectively suppressed, reducing rainfall by ~50%: the first 17 days of May were rain-free, for example, and the monthly precipitation total exceeded 3 cm at only one station, St. Petersburg, and fell nearly all on one day, 19 May.

Fig. 1 shows the locations of the 915 MHz radar profiler + RASS (radio acoustic sounding system) instruments installed at the Sydney (SN) supersite, at Ruskin (RK), south of Sydney and nearer to the Bay, and in St. Petersburg (SP) on the west side of the Bay. For additional information on the profiler + RASS instrumentation and data see NOAA–ETL (http://www.etl.noaa.gov/et7/data/archive/EditedNonActive/index.html). Profiler + RASS data were used together with data from the 00:00 and 12:00 UTC (20:00 and 08:00 LT) soundings at local airports to determine the structure of the planetary boundary layer (PBL); mixing layer depths at Sydney, for example, were often observed in excess of 2000 m by 16:00 LT (see Gunter (this issue), for a detailed discussion of the boundary layer characteristics). The profiler + RASS data were also used to segregate days into one of four categories as a function of synoptic or sea- and bay-breeze winds. Table 1 shows that 19 days were dominated by strong or transitional synoptic flow with no local effects. Of the remaining days, five were classed as strong sea-breeze events, with the wind change seen at all three profiler stations and return flow indicated, and 6 days saw weak sea-breeze events, defined as having surface winds other than due West, wind change not observed at all profiler stations (usually missing from the site farthest inland at Sydney), and no return flow. On average, the sea-breeze fronts arrived at Ruskin, for example, between 12:00 and 13:00 LT, reached a maximum depth of 1000 m, and dissipated between 20:00 and 21:00 LT.

Fig. 1. Satellite depiction of the Tampa, FL, environment with profiler + RASS sites indicated: SP, St. Petersburg; RK, Ruskin; SN, Sydney.

Table 1
Meteorological regimes in May, 2002

Days
1^{SS} | 2^{SS} | 3^{SSB} | 4^{SSB} | 5^{SWS} | 6^{SWS} | 7^{WSB} | 8^{WSB} | 9^{SSB} | 10^{WSB} | 11^{SS} | 12^{WSB} | 13^{SWS} 14^{SWS} | 15^{SS} | 16^{WSB} | 17^{SWS} | 18^{SS} | 19^{R} | 20^{SWS} | 21^{SWS} | 22^{SS} | 23^{SS} | 24^{SS} | 25^{SS} 26^{SS} | 27^{SS} | 28^{SS} | 29^{SSB} | 30^{SSB} | 31^{WSB}

[SS] Strong Synoptic: synoptic flow dominates all local effects. Total: 12 days.
[SWS] Synoptic Wind Shift: wind shift forced by synoptic features. Total: 7 days.
[SSB] Strong Sea Breeze: wind shift due to local effects of sea or bay breeze. Strong when surface winds were due West; wind change was observed at all three profiler stations; and return flow was indicated. Total: 5 days.
[WSB] Weak Sea Breeze: weak when surface winds were not due West; wind change was not observed at all three profiler stations; and no return flow was indicated. Total: 6 days.
[R] Rain. Total: 1 day.

3.2. Chemical environment in May 2002

3.2.1. Gas-phase constituents

Fig. 2 shows variations with altitude in the mixing ratios of O_3, NO and NO_2, NO_Y (NO_Y = the sum of all oxidized N compounds) and NO_Z ($NO_Z = NO_Y - NO_X$), and the ratio of NO_Z to NO_Y using 30 min averages of the 1 Hz measurements of these gas-phase species corresponding to the 30 min period of FP loading for the aerosol samples. In each case, the 57 total 30 min samples were segregated by location of the aircraft during

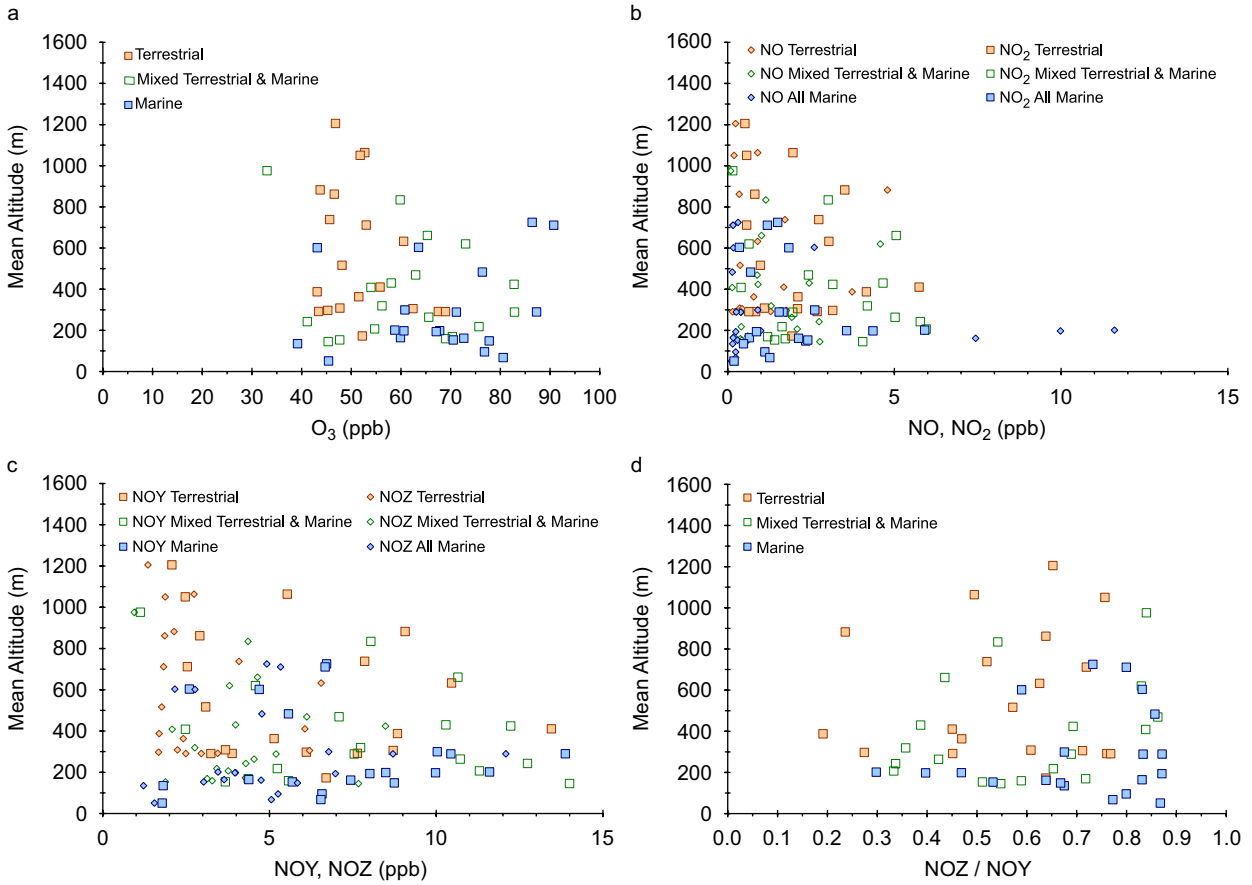

Fig. 2. (a) O_3 mixing ratio during Twin Otter aerosol sampling as a function of mean altitude. Samples are segregated for flights over marine, terrestrial, and mixed marine and terrestrial land use. (b) Same as (a) except for NO and NO_2. (c) Same as (a) except for NO_Y and NO_Z. (d) Same as (a) except for the ratio NO_Z/NO_Y.

the sample period: either entirely over land ("terrestrial"), entirely over the Gulf of Mexico or Tampa Bay ("marine"), or over portions of land and water ("mixed"). These samples are not entirely discrete vertically since the aircraft did not always maintain straight and level flight for all of each 30 min FP sample loading period. Deviations were small, however, most often less than 50 m, and the data thus are coherent representations of atmospheric conditions. The lower limit for O_3 (Fig. 2a) from these samples was consistent throughout the PBL at ~40 ppb. The highest $[O_3]$, >80 ppb, were observed with marine and mixed samples very likely because more of these samples were collected nearer to NO_X sources at the surface where the greatest $P(O_3)$ occurs, and because physical losses to surfaces are reduced over water. Mixing ratios of NO and NO_2 (Fig. 2b) show the expected fall-off with increasing altitude, and these data, together with the profiler + RASS data, indicate that the data set was well-mixed up to ~700 most days. In addition, terrestrial $[NO_Y]$ (Fig. 2c) was roughly invariant with mean altitude at 1–3 ppb. Fig. 2d shows that the freshest plumes—those with lowest $[NO_Z]/[NO_Y]$ ratios—at all altitudes were found in the terrestrial samples nearer to the NO_X sources.

The urban and marine mixed layers of the lower troposphere were largely well-mixed during May 2002 as demonstrated by the mostly invariant $[NO_Y]$ up to ~700 m (Fig. 2c). However, heterogeneity in the aerosol samples might have been expected as a result of inadvertent sampling when the aircraft encountered intense power plant plumes. Such sampling would have been inadvertent because while several aircraft missions were devoted to characterizing power plant plumes, aerosol sampling was generally not performed during these times. The ratio of $[SO_2]$ to $[NO_Y]$ shown in Fig. 3

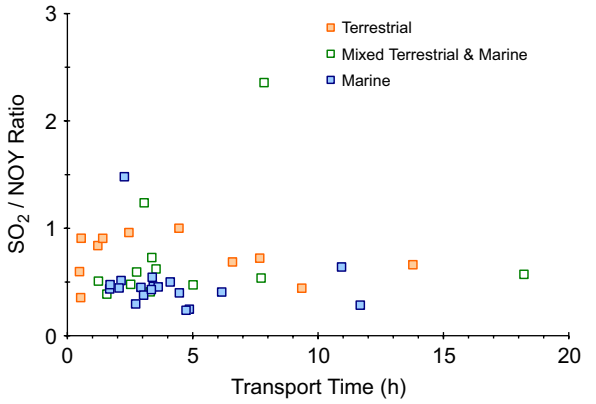

Fig. 3. Ratio of SO_2/NO_Y as a function of plume transport time from the Tampa urban core.

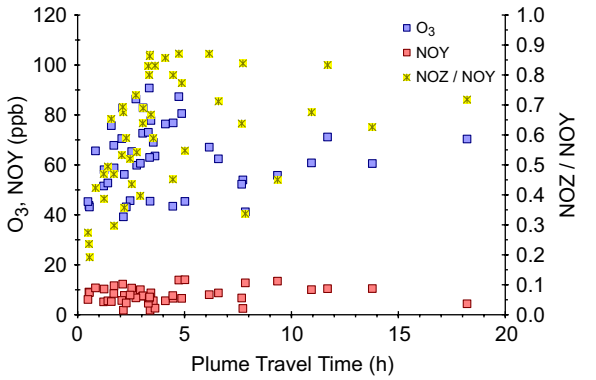

Fig. 4. Mixing ratios of O_3 and NO_Y (left axis), and the ratio of NO_Z/NO_Y (right axis) as a function of plume transport time from the Tampa urban core.

was largely stable with a value <1 over nearly all hours of plume travel time (travel time being computed from the aircraft's mean distance from Tampa and the vector average wind speed during the sample periods). Because power plant plumes are substantially enriched in SO_2 relative to urban plumes dominated by mobile source emissions, the consistently low value of this ratio demonstrates that the samples used in this analysis were mostly free of contamination from power plant plume air masses. The single marine and two mixed samples with an $[SO_2]/[NO_Y]$ ratio >1 were all from afternoon flights on 30 or 31 May, days when a general stagnation event settled over Tampa and the power plant plumes became so completely commingled with the urban and marine chemistry that separation for isolated aerosol sampling was not possible. The mean $[SO_2]$ (not shown) for all samples except those three on 30 and 31 May was 3.47 ppb, while the $[SO_2]$ for those three samples was greater than that mean by a factor of 4 to 5. Hence, we conclude that this aerosol data set is coherent and that comparisons can usefully be made across days to characterize the urban and marine influence in the Tampa airshed.

Fig. 4 shows that $P(O_3)$ and NO_X conversion to NO_Z were largely complete in the Tampa urban plumes in <5 h and that total NO_Y was conserved throughout the plumes over time, as expected.

3.2.2. *Aerosol-phase constituents*

Total inorganic aerosol mass concentration in terrestrial, marine, and mixed samples was dominated by anion constituents in both fine- and coarse-mode fractions as summarized in Table 2. For fine-mode particles, the mean anion mass concentration was more than a factor of 2 greater than the mean cation mass concentration, while coarse-mode mean anion mass concentration exceeded mean cation mass concentration by more than 50% for all locations. Table 2 also shows that the mean of the total mass concentration in the terrestrial samples was $>30\%$ lower than in marine or mixed sample totals and that most of this difference occurred in the fine-mode fraction. Fig. 5a–c shows mass concentration values for fine- and coarse-mode aerosols in the terrestrial (Fig. 5a), marine (Fig. 5b), and mixed (Fig. 5c) samples from each flight. Mixed and marine samples tended to be dominated by fine-mode aerosols while mean mass concentration totals for the terrestrial samples were more nearly equal across aerosol size: 3.1 $\mu g\,m^{-3}$ in the coarse-mode vs. 3.9 $\mu g\,m^{-3}$ in the fine mode.

Table 2
Mean mass concentrations

	Cations ($\mu g\,m^{-3}$)	Anions ($\mu g\,m^{-3}$)	Total ($\mu g\,m^{-3}$)
Coarse-mode fraction			
Terrestrial	1.1	2.0	3.1
Marine	1.2	2.3	3.5
Mixed	1.2	2.2	3.4
Fine-mode fraction			
Terrestrial	1.2	2.6	3.8
Marine	2.1	4.7	6.8
Mixed	2.1	5.1	7.2
Total			
Terrestrial	2.4	4.6	7.0
Marine	3.3	7.0	10.3
Mixed	3.3	7.4	10.7

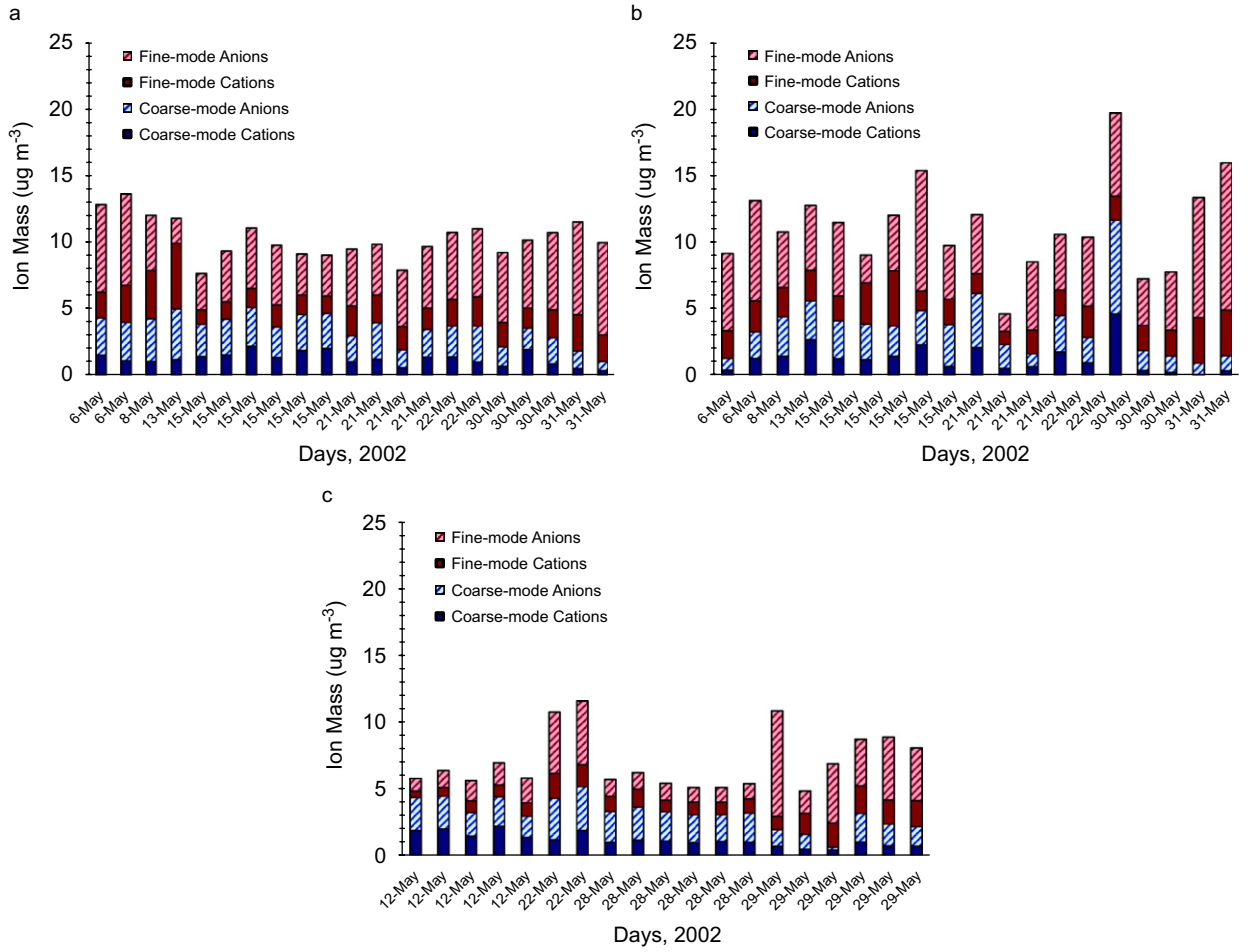

Fig. 5. (a) Ion mass concentrations for each sample every day taken over marine land use by ion type and size fraction. (b) Same as (a) except for mixed terrestrial and marine land use. (c) Same as (a) except for terrestrial land use.

This mean, however, was dominated by outlier totals from four flights, two on 22 May and two on 29 May; coarse-mode mass dominated the terrestrial samples in nearly all the remaining 15 flights.

Fig. 6a–c summarizes the size- and species-segregated mass concentration data in cumulative probability plots for the coarse-mode mass (Fig. 6a), and fine-mode mass (Fig. 6b–c). Mass in the fine-mode fraction was dominated by SO_4^{2-} and NH_4^+ with SO_4^{2-} mass exceeding NH_4^+ mass by at least a factor of 2 and often by a factor of 4 or more. This coheres with the mean mass concentration fractions for anions and cations in Table 2 and suggests that $(NH_4)_2SO_4$ and NH_4HSO_4 were responsible for most of the fine-mode aerosol mass even in these samples taken for the most part outside of direct power plant plumes (see Fig. 3 and discussion above for power plant plume exclusion). Coarse-mode inorganic mass concentration was dominated by Na^+, Cl^- and NO_3^-, suggesting that coarse-mode aerosols in these samples from all locations were dominated by NaCl and $NaNO_3$, potentially as a result of Cl^- replacement as in (R5) above. Coarse-mode aerosols also showed a high quantity of Ca^{2+} and K^+, suggesting contributions from road dust and biomass burning sources that together often exceeded the cationic contribution from sea salt. Table 3 lists the daily mean concentrations of the coarse-mode fraction Na^+, non-sea salt Ca^{2+}, and K^+, and the ratio of the sum of non-sea salt Ca^{2+} and K^+ to Na^+. Magnesium ion was also found in these samples, chiefly in the coarse-mode fraction, but at mass concentrations nearly all $<0.2\,\mu g\,m^{-3}$.

While the anions NO_3^-, Cl^-, and SO_4^{2-} dominated both coarse- and fine-mode inorganic particle mass,

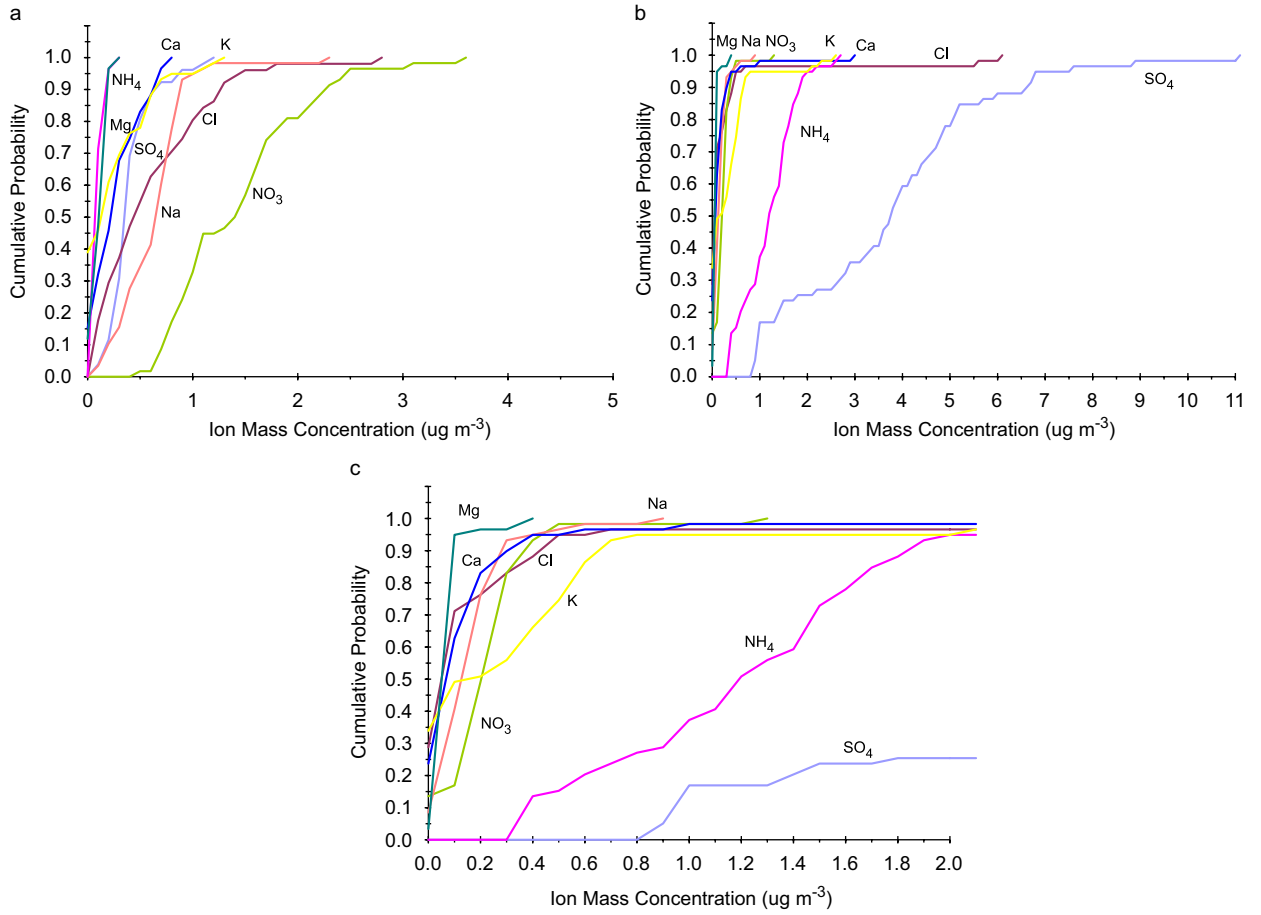

Fig. 6. (a) Cumulative probabilities of coarse-mode ion mass concentrations for measured cations and anions. (b) Same as (a) except for fine-mode aerosols. (c) Same as (b) except at finer concentration scale.

an ion balance analysis shows that particles of both modes were nearly in charge balance. Fig. 7 shows the ion difference computed on a μ equivalent basis as the difference in total cations minus total anions and plotted against the ion μ equivalent totals for coarse- and fine-mode samples. No trend is apparent with either size distribution and >85% of the differences are <0.05 μ equivalents. Table 4 lists the mean and ranges of the ratio of the difference from total cation minus total anion to the ion total μ equivalent for each size distribution and for each location. On a μ equivalent basis, cations clearly dominated each mode and all sample locations, but the mean differences were <10% in all cases except for the fine-mode terrestrial samples where cations dominated by >12%, and for the coarse-mode marine samples where cations dominated by ~14%. Overall, fine-mode aerosols were slightly alkaline by ~5% and coarse-mode aerosols by ~10%. It is of course possible that this apparent slight cation equivalent excess is an artifact of having missed collecting on the FP a range of aerosol anion species. Tabazadeh et al. (1998) speculated, for example, that such missing anions were likely to be higher organic acids not retained on the filter face in sufficient quantities for analysis. Because the particles are so nearly in charge balance, however, the contribution of any potentially missing aerosol-sourced anions in this case would be slight.

4. Interpretation and discussion

4.1. Chemical form and distribution of NO_3

Although NO_3 can also be present in peroxyacetyl nitrate (PAN) and other higher organic nitrates, for the 2002 Twin Otter missions, total NO_3 is defined as the sum of the measured fine- and

Table 3
Mean coarse-mode fraction Na^+, Ca^{2+}, and K^+ by mission

Sample day	Location	Na^+ ($\mu g\,m^{-3}$)	Ca^{2+} ($\mu g\,m^{-3}$)	K^+ ($\mu g\,m^{-3}$)	$(Ca^{2+}+K^+)$ ($\mu g\,m^{-3}$)	$(Ca^+ + K^+)/Na^+$ ($\mu g\,m^{-3}$)
6 May	Marine	0.7	0.2	0.1	0.3	0.4
	Mixed	0.8	0.3	0.1	0.4	0.4
8 May	Marine	0.9	0.0	0.0	0.0	0.0
	Mixed	0.7	0.5	0.5	1.1	1.4
10 May	Mixed	0.6	0.5	0.0	0.5	0.8
12 May	Terrestrial	0.6	0.4	0.6	0.9	1.5
13 May	Marine	0.7	0.0	0.5	0.5	0.7
	Mixed	0.8	0.3	0.3	0.7	0.8
15 May	Marine	0.7	0.6	0.3	0.9	1.3
17 May	Mixed	0.5	0.0	0.0	0.0	—
21 May	Marine	0.6	0.2	0.1	0.3	0.5
	Mixed	0.1	0.1	0.4	0.4	3.6
	Terrestrial	1.0	0.2	0.2	0.3	0.4
22 May	Marine	0.7	0.0	0.5	0.4	0.7
	Mixed	0.6	0.4	0.2	0.7	1.1
28 May	Terrestrial	0.8	0.1	0.1	0.2	0.2
29 May	Terrestrial	0.4	0.1	0.1	0.2	0.4
30 May	Marine	0.4	0.3	0.4	0.6	1.8
	Mixed	2.2	0.7	1.3	2.0	0.9
31 May	Marine	0.1	0.1	0.3	0.4	**3.9**

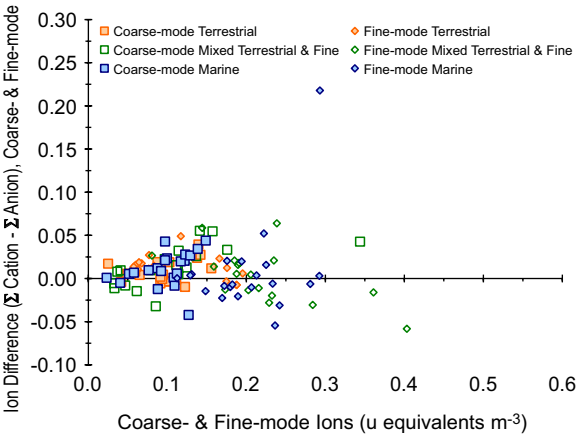

Fig. 7. Ion charge balance, cations minus anions, for coarse- and fine-mode aerosol fractions segregated by land use type vs. coarse- and fine-mode ion mass equivalents.

coarse-mode aerosol NO_3^- and the gas-phase HNO_3. Fig. 8 shows the concentration distribution with altitude of these three NO_3 forms. Total NO_3 in all samples was strongly dominated by HNO_3 which reached a concentration maximum of 10–16 $\mu g\,m^{-3}$ between 200 and 400 m. Since no differences by location were apparent in this trend, this vertical layer presumably represents a point of balance between surface-sourced HNO_3 production in the urban plume and physical loss by deposition which would be maximized nearer to ground. Aerosol NO_3 was found predominately in the coarse-mode fraction at all altitudes and was largely invariant above 200 m at ~1.4 $\mu g\,m^{-3}$. All samples below 200 m shown in Fig. 8 were taken over marine locations and were slightly enhanced in NO_3 relative to the terrestrial and mixed samples. This coheres with the observation drawn from Fig. 2 above that these low-altitude marine samples had been processed further than the terrestrial ones, evidenced by their greater chemical age (Fig. 2d) and higher $[O_3]$ (Fig. 2a). This is likely due to vertical shear in the atmosphere whereby an early-formed, well-mixed plume drifts westward from the Tampa urban core on the predominating off-shore flow and becomes striated once over the Gulf due to changes in the surface heat flux input over water. The striation allows NO_X processing in the low-level near-surface component of the plume to continue in a now substantially reduced atmospheric volume. Fine-mode $[NO_3^-]$ was stable throughout the PBL at a very low level with a mean of 0.2 $\mu g\,m^{-3}$, or ~15% of the coarse fraction mean. Fig. 9 shows the percent contributions to total NO_3 from each aerosol size fraction and from HNO_3. This display coheres well with the data in Fig. 8, confirming both that HNO_3 dominated total $[NO_3]$ and that fine-mode NO_3^- was persistently present but never

Table 4
Mean differences of the sum of cations minus the sum of anions, and ratioed to the ion total

	(Σ cations–Σ anions)/ion total (μ equivalents)		
	Min	Max	Mean
Coarse-mode fraction			
Terrestrial	−0.1	0.3	0.1
Marine	−0.1	0.4	0.1
Mixed	−0.4	0.3	0.1
Overall, all locations	−0.4	0.4	0.1
Fine-mode fraction	−0.6	0.7	0.1
Terrestrial	−0.6	0.4	0.1
Marine	−0.2	0.7	0.0
Mixed	−0.5	0.4	0.0
Overall, all locations	−0.6	0.7	0.1

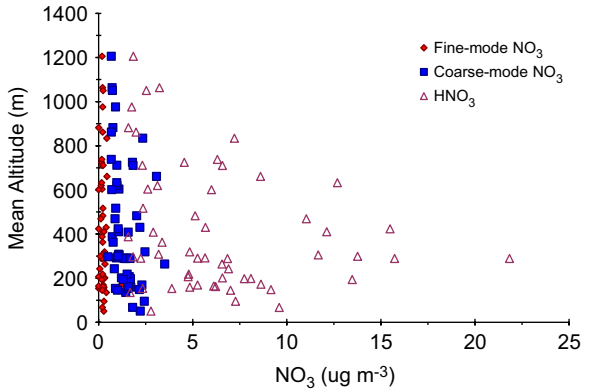

Fig. 8. NO_3 mass concentrations segregated by size fraction and with gas-phase HNO_3 as a function of mean altitude.

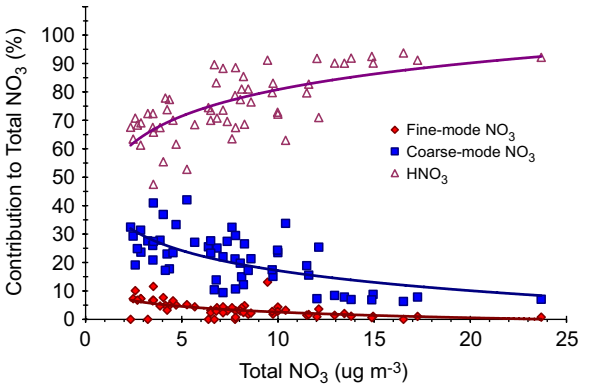

Fig. 9. Percent contribution to total NO_3 from coarse- and fine-mode aerosol fractions and from gas-phase HNO_3.

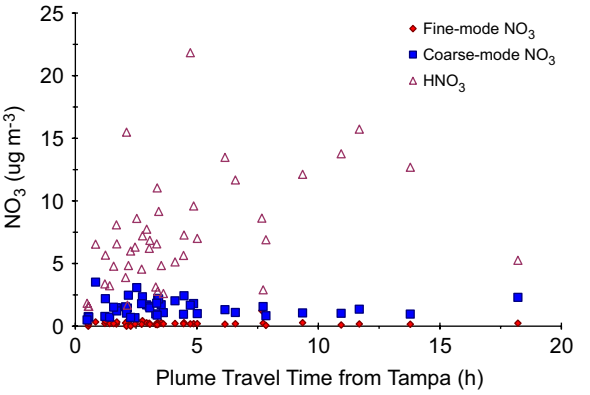

Fig. 10. Same as Fig. 9 except as a function of plume travel time.

contributed >15% to total NO_3 with a mean contribution of <4%. In fact, as Fig. 10 shows, only HNO_3 accumulated as the urban plume aged, while fine- and coarse-mode NO_3 each appear to have been in a rough equilibrium of production and loss even after the first 4 h of highest HNO_3 production.

The substantial [HNO_3] in these samples relative to the measured aerosol [NO_3^-] makes it possible that HNO_3 could have been adsorbed to aerosols on the filter face in quantities sufficient to enhance the reported [NO_3^-] as an artifact in either or both size fractions. If this sampling artifact were present, we might expect that it would be positively correlated with [HNO_3]. However, Fig. 11 shows that while a strong correlation with [HNO_3] held for total [NO_3] ($R^2 = 0.97$), dominated as it is by HNO_3, no correlation held for either coarse- ($R^2 = 0.02$) or fine-mode ($R^2 = 0.00$) [NO_3^-], meaning that the measured [NO_3^-] reported in these samples is unlikely to have been a filter-based artifact from high [HNO_3].

4.2. Coarse-mode Cl^- replacement and NO_3^- uptake

The presence of NO_3^- on coarse-mode aerosols is generally explained by uptake of HNO_3 and replacement of Cl^- from the prevalent sea salt NaCl as described above. Hence, Cl^- depletion on coarse-mode particles can be calculated as the remainder when the [Cl^-] measured on the coarse-mode particle is subtracted from the original [Cl^-]. However, original [Cl^-] is not a measured quantity but must be computed from the measured coarse-mode [Na^+] and the assumed original ratio of [Cl^-] to [Na^+] in sea salt aerosols, 1.174 (Zhang

et al., 1999). Hence,

$$Cl^- \text{ depletion} = 1.174[Na^+]_{meas} - [Cl^-]_{meas.} \quad (1)$$

Fig. 12a shows that coarse-mode Cl^- depletion increased with plume travel time and could reach 100% replacement in <4 h. (Note that not all samples here have an associated plume travel time because wind speed estimates were not available for all aerosol sampling times.) The urban plumes encountered over Tampa Bay or the Gulf of Mexico were more depleted in coarse-mode Cl^- than those over land when sampled in the first 4 h, and consequently reached full Cl^- replacement earlier than the terrestrial plumes. In contrast to the relation with plume travel time, coarse-mode Cl^- depletion vs. chemical age using the ratio NO_Z/NO_Y (Fig. 12b) shows no correlation for terrestrial or mixed samples (R^2 <0.05), but a weak positive correlation for the marine samples ($R^2 = 0.33$). Also, only four of 18 terrestrial samples had Cl^- depletion totals >50% while all marine samples did. This dichotomy might be explained by the difference in sources for the two components of this index. NO_X, the source of the terms in the chemistry ratio used to indicate aging here, comes almost exclusively from the Tampa urban area, while sea salt, the Cl^- source and site for NO_3^- substitution, comes from Tampa Bay and the Gulf of Mexico. Marine samples of the urban plume were encountered mostly west of the Tampa urban core over the Gulf of Mexico and would therefore have had greater opportunity for mixing HNO_3, present in the NO_Z total now aged over several hours travel time from the emitted urban NO_X, with sea salt emissions. Recall also that marine samples were predominately more aged than terrestrial ones, both in absolute terms as Fig. 2c shows and relative to NO_Y as Fig. 2d shows. Nitric acid in these aged, low-level urban plumes would have had increased opportunity for NO_3^- substitution with the fresh sea salt from the water surface.

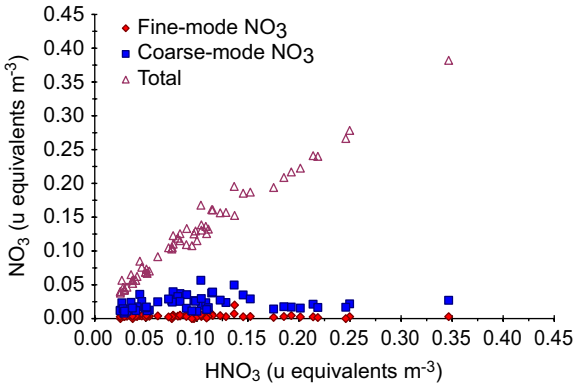

Fig. 11. NO_3 μ equivalent concentration segregated by size fraction and with total NO_3 as a function of HNO_3 concentration.

The stoichiometry of (R5) suggests that a 1:1 correspondence should hold between μ equivalent measures of coarse-mode $[NO_3^-]$ and coarse-mode Cl^- depletion. Fig. 13 shows the actual relationship between these two and for fine-mode aerosols as well. Because NO_3 and NaCl were preferentially present in the coarse fraction as expected from the relative ion mass concentrations (see Figs. 6a–c and 9), a

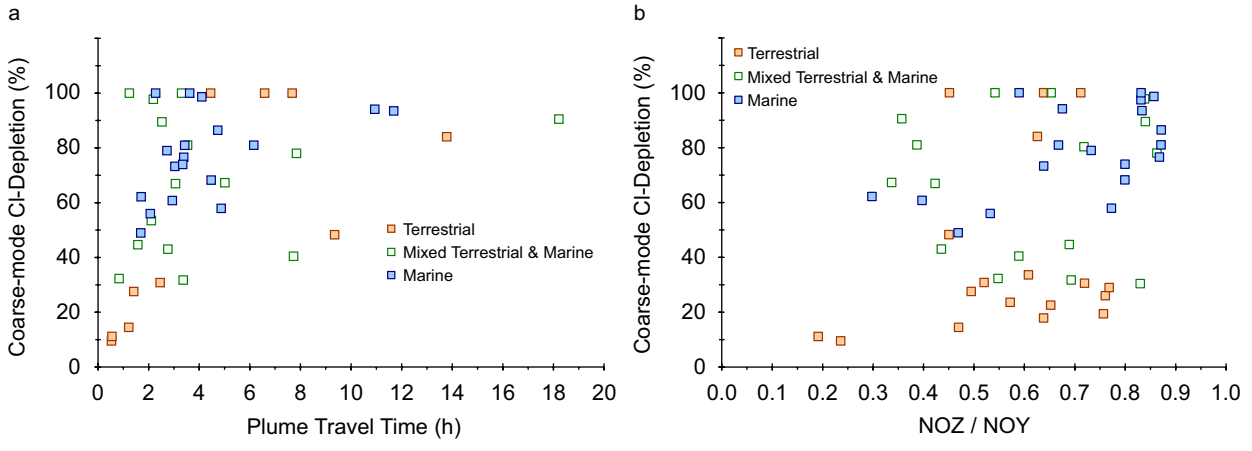

Fig. 12. (a) Coarse-mode Cl^- depletion as a function of plume travel time and segregated by land use type. (b) Coarse-mode Cl^- depletion as a function of photochemical age using the indicator NO_Z/NO_Y and segregated by land use type.

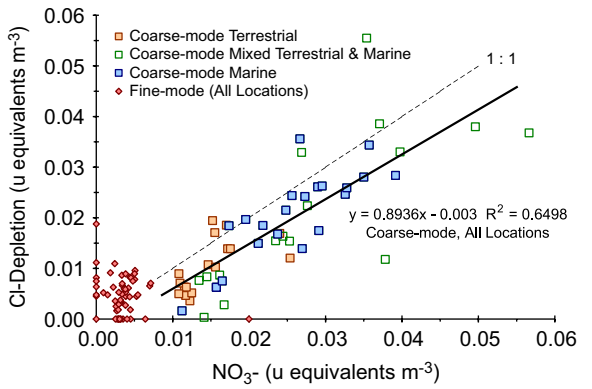

Fig. 13. Fine- and coarse-mode Cl^- depletion as a function of NO_3^- concentration with regression fit (solid line) and 1:1 correspondence (dashed line).

correspondence holds only for the large aerosols. However, that correspondence shows variation from theoretical unity.

High Cl^- depletion—i.e., above the dashed 1:1 line in Fig. 13—might be explained through surface aerosol reaction of acid gases other than HNO_3, of H_2SO_4, for example (Chameides and Stelson, 1992; Zhang et al., 1999), or from oxidation of SO_2 to SO_4^{2-} by O_3 or H_2O_2 on the aerosol surface (Keene et al., 1998). All of these products were present in the aged urban air masses encountered over Tampa in 2002.

Low Cl^- depletion—i.e., below the dashed 1:1 line in Fig. 13 where most of the coarse-mode data points lie—might be explained by retention on the particle of the HCl formed from NO_3^- substitution. Although pH measurements are not available for these samples in 2002, the pH of fresh sea salt particles is generally assumed to be ~8 and to increase as the particles age and undergo evaporation (Keene et al., 1998). Alkalinities in this range make it plausible that HCl would be retained on the coarse particles; moreover, recall that these particles were separately estimated to be slightly out of charge balance in favor of the cations (see Fig. 7 and Table 4 above).

A more direct indicator of the availability of NO_3^- for Cl^- replacement can be computed as the mean ratio of $[HNO_3]$, the likely source of coarse-mode NO_3^-, to the coarse-mode $[Na^+]$. On a μ equivalent basis for the coarse-mode particles, this ratio was on the order of only a factor of 5, while the mean ratio of coarse-mode $[NO_3^-]$ to coarse-mode $[Na^+]$ for all sample locations was ~0.85. Thus it seems plausible that NO_3^- and its HNO_3 progenitor were not present in the Tampa airshed in sufficient amounts to titrate fully the slightly alkaline coarse-mode particles. This would allow these aerosols to retain the HCl resulting from the partial NO_3^- substitution and reduce the value of Cl^- depletion. In Tampa, the values were ~11% on average below theoretical unity (see Fig. 13). Secondarily, NO_3^- may be so limited that not all available Cl^- from NaCl in the coarse fraction can be replaced, leaving NaCl intact on the particles and thus further reducing the calculated Cl^- replacement value. This explanation requires that the Na^+ on the coarse particles be associated exclusively with either Cl^- or NO_3^-, and that appears to have been borne out. Fig. 14 shows that the slope of coarse mode $[Na^+]$ to coarse mode $[NO_3^-]$ was 0.81, slightly less than the value of 0.85 expected from the original ratio of $[Na^+]$ to $[Cl^-]$ and assuming full Cl^- replacement. Because the slope of coarse mode $[Na^+]$ to the sum of coarse mode $[NO_3^-]$ and $[Cl^-]$ was 0.85 (not shown in Fig. 14), it seems reasonable that most of the Cl^- not replaced by NO_3^- on coarse particles remained bound to Na^+. Additional support for the hypothesis of NO_3^- limitation is derived from the enhanced $[Na^+]$ in terrestrial samples relative to marine and mixed ones as shown in Fig. 14. This then coheres with the lower value of Cl^- depletion in the terrestrial samples relative to the mixed and marine ones as shown in Fig. 12b, and with the lower $[HNO_3]$ for terrestrial samples overall shown in Fig. 15. The mean $[HNO_3]$ in terrestrial samples, for example, was 4.8 vs. 6.1 $\mu g\,m^{-3}$ and 7.9 $\mu g\,m^{-3}$ in the mixed and marine samples, respectively.

4.3. Potential for other mechanisms of coarse-mode NO_3 formation

Given the high mass concentrations of non-sea salt Ca^{2+} and K^+ found on the particles from Tampa (see Fig. 6 and Table 3), it is possible that these cations played a role in addition to that of NaCl in sequestering NO_3^- from HNO_3 on coarse-mode aerosols. Hanisch and Crowley (2001a, b) measured a high and irreversible uptake coefficient (γ) for HNO_3 to authentic mineral dust samples of 0.1, and showed enhanced HNO_3 uptake to $CaCO_3$ in the presence of water vapor (2001a) which might suggest additional enhancement in the Tampa airshed. The overall effect of this uptake by Ca^{2+} and K^+ would be small, however, and, extrapolating for the non-sea salt Ca^{2+} and K^+ mass

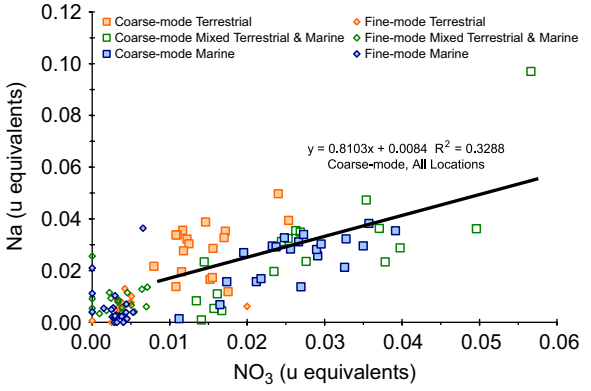

Fig. 14. Na^+ μ equivalent concentration vs. NO_3^- μ equivalent concentration for coarse- and fine-mode aerosol fractions and segregated by land use type. Regression fit to the coarse-mode fraction is shown for all land use types.

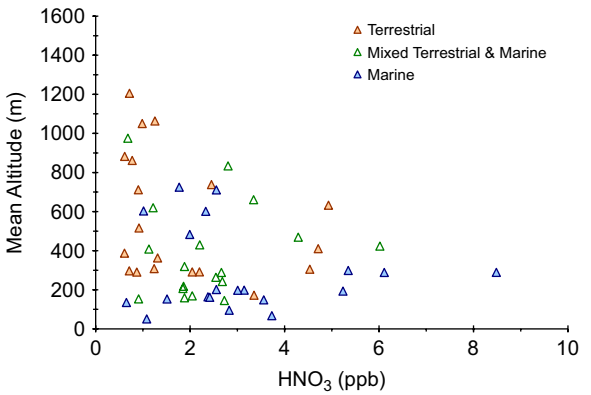

Fig. 15. HNO_3 mixing ratio as a function of mean altitude and segregated by land use type.

concentrations measured at Tampa in 2002, we calculate that these mineral dust constituents can have removed only $\sim 0.05\,\mu g\,m^{-3}$ HNO_3.

5. Conclusions

The distributions of inorganic mass concentrations of both fine- and coarse-mode aerosol fractions in Tampa during May 2002 were dominated by anions, SO_4^{2-} in the fine-mode fraction and Cl^- and NO_3^- in the coarse-mode fraction. Sodium ion was the predominate cation in the coarse-mode fraction, although non-sea salt Ca^{2+} and K^+ were present in amounts that together equaled or surpassed the $[Na^+]$. Ion balance calculations show that the particles were for the most part nearly in charge balance, although cations slightly predominated in both size fractions. Although total NO_3 was dominated by HNO_3, it appears from our coarse-mode Cl^- depletion calculations and from the supporting evidence of particle alkalinity, that NO_3^- and HNO_3 were not present in the Tampa airshed in sufficient amounts to titrate fully the slightly alkaline coarse-mode particles there and to replace fully the Cl^- associated originally with Na^+.

Acknowledgments

We thank our colleagues in the NOAA Air Resources Laboratory and in the Aircraft Operations Division, particularly Mr. Dennis Wellman and LT Phil Hall, aircraft commander for the BRACE missions. We also acknowledge the help of Mr. Paul Tate at USF with sample analysis are especially grateful to Dr. Thomas Atkeson, the BRACE program manager at the Florida Department of Environmental Protection, for his thoughtful and generous support.

Disclaimer: The research presented here was performed under the Memorandum of Understanding between the US Environmental Protection Agency (USEPA) and the National Oceanic and Atmospheric Administration (NOAA) of the US Department of Commerce, and under agreement number DW13921548. This work constitutes a contribution to the NOAA Air Quality Program. Although it has been reviewed by USEPA and NOAA and approved for publication, it does not necessarily reflect the policies or views of either agency. Mention of trade names or manufacturers does not imply endorsement.

References

Atkeson, T., Greening, H., Poor, N., 2007. The Tampa Bay Regional Atmospheric Chemistry experiment (BRACE). Atmospheric Environment, this issue.

Andreae, M.O., Crutzen, P.J., 1997. Atmospheric aerosols: biogeochemical sources and role in atmospheric chemistry. Science 276, 1052–1058.

Chameides, W.L., Stelson, A.W., 1992. Aqueous-phase chemical processes in deliquescent sea salt aerosols: a mechanism that couples the atmospheric cycles of S and sea salt. Journal of Geophysical Research 97 D14, 20565–20580.

Clarke, A.J., Azadi-Boogar, G.A., Andrews, G.E., 1999. Particle size and chemical composition of urban aerosols. Science of the Total Environment 235, 15–24.

De Haan, D.O., Brauers, T., Oum, K., Stutz, J., Nordmeyer, T., Finlayson-Pitts, B.J., 1999. Heterogeneous chemistry in the troposphere: experimental approaches and applications to the

chemistry of sea salt particles. International Review of Physical Chemistry 18 (3).

Duce, R.A., Liss, P.S., Merrill, J.T., Atlas, E.L., Baut-Menard, P., Hicks, B.B., Miller, J.M., Prospero, J.M., Arimoto, R., Church, T.M., Ellis, W., Galloway, J.N., Hansen, L., Jickells, T.D., Knap, A.H., Reinhardt, K.H., Schneider, B., Soudire, A., Tokos, J.J., Tsunogai, S., Wollash, R., Zhou, M., 1991. The atmospheric input of trace species to the world ocean. Global Biogeochemical Cycles 5, 193–259.

FDEP, 2002. The Florida Department of Environmental Protection. Air Quality Maintenance Plan (2005–2015): Hillsborough and Pinellas Counties Florida. Department of Environmental Protection, Division of Air Resource Management, Florida.

Fisher, D.C., Oppenheimer, M., 1991. Atmospheric nitrogen deposition and the Chesapeake Bay estuary. Ambio 20, 102–108.

Galloway, J.N., Aber, J.D., Erisman, J.W., Seitzinger, S.R., Howarth, R.W., Cowling, E.B., Cosby, B.J., 2003. The nitrogen cascade. Bioscience 53, 341–356.

Guelle, W., Schultz, M., Balkanski, Y., Dentener, F., 2001. Influence of the source formulation on modeling the atmospheric global distribution of sea salt aerosol. Journal of Geophysical Research 106 D21, 27509–27524.

Gunter, L., Assessment of boundary layer variations in the Tampa Bay area during BRACE. Atmospheric Environment, this issue.

Hanisch, F., Crowley, J.N., 2001a. Heterogeneous reactivity of gaseous nitric acid on Al_2O_3, $CaCO_3$, and atmospheric dust samples: a Knudsen cell study. Journal of Physical Chemistry A 105, 3096–3106.

Hanisch, F., Crowley, J.N., 2001b. The heterogeneous reactivity of gaseous nitric acid on authentic mineral dust samples, and on individual mineral and clay mineral components. Physical Chemistry Chemical Physics 3, 2474–2482.

Howarth, R., Anderson, D., Cloem, J., Elfring, C., Hopkinson, C., Lapointe, B., Malone, T., Marcus, N., McGlathery, K., Sharpley, A., Walker, D., 2000. Nutrient pollution of coastal rivers, bays, and seas. Issues in Ecology 7, 1–15.

Jaworski, N.A., Howarth, R.W., Hetling, L.J., 1997. Atmospheric deposition of nitrogen oxides onto the landscape contributes to coastal eutrophication in the Northeast United States. Environmental Science and Technology 31 (7), 1995–2004.

Keene, W.C., Sander, R., Pzenny, A.A.P., Vogt, R., Crutzen, P.J., 1998. Aerosol pH in the marine boundary layer: a review and model evaluation. Journal of Aerosol Science 29, 339–356.

Luke, W., Arnold, J., Gunter, L., Watson, T., Wellman, D., Dasgupta, P., Li, J., Riemer, D., Tate, P., 2006. The NOAA Twin Otter and its role in BRACE: platform description. Atmospheric Environment, this issue.

Mamane, Y., Mehler, M., 1987. On the nature of nitrate particles in a coastal urban area. Atmospheric Environment 21 (9), 1989–1994.

Paerl, H.W., 1995. Coastal eutrophication in relation to atmospheric nitrogen deposition: current perspectives. Ophelia 41, 237–259.

Paerl, H.W., 1997. Coastal eutrophication and harmful algal blooms: Importance of atmospheric deposition and groundwater as "new" nitrogen and other nutrient sources. Limnology and Oceanography 42, 1154–1165.

Prible, J.R., Janicki, A.J., Greening, H. (Eds.), 2003. Bay Wide Environmental Monitoring Report, 1998–2001 Tampa Bay National Estuary Program, Tampa, FL.

Poor, N., Pribble, J.R., Greening, H., 2001. Direct wet and dry deposition ofammonia, nitric acid, ammonium, and nitrate to the Tampa Bay Estuary, FL, USA. Atmospheric Environment 35, 3947–3955.

Pryor, S.C., Sørensen, L.L., 2000. Nitric acid-sea salt reactions: implications for nitrogen deposition to water surfaces. Journal of Applied Meteorology 39, 725–731.

Tabazadeh, A., Jacobson, M.Z., Singh, H.B., Toon, O.B., Lin, J.S., Chatfield, R.B., Thakur, A.N., Talbot, R.W., Dibb, J.E., 1998. Nitric acid scavenging by mineral and biomass burning aerosols. Geophysical Research Letters 25, 4185–4188.

UNEP, 2004. United Nations Environment Programme, Global Environment Outlook Year Book 2003, (http://www.unep.org/geo/yearbook/).

Zhang, H., Chan, C.K., Fang, M., Wexler, A.S., 1999. Formation of nitrate and non-sea salt sulfate on coarse particles. Atmospheric Environment 33, 4223–4233.